# Drift volume in viscous flows

Nicholas G. Chisholm and Aditya S. Khair*
*Department of Chemical Engineering, Carnegie Mellon University, 5000 Forbes Avenue, Pittsburgh, Pennsylvania 15213, USA*
(Received 2 March 2017; published 9 June 2017)

The drift volume $D$ refers to the volume of fluid enclosed between the initial and final profiles of an initially flat marked sheet of fluid that deforms due to the passage of a body. Classic investigations of the drift volume in an inviscid fluid show that $D$ is comparable in magnitude to the volume of the translating body. The situation is fundamentally different for a viscous fluid. For instance, if the Reynolds number Re is zero, then $D$ diverges with the distance traveled by the body and is typically orders of magnitude larger than the body volume. The goal of the present paper is to quantify the drift volume when Re is finite. We interpret the drift volume as the flux through a stationary plane bounded by a stream tube, thus allowing $D$ to be computed without explicit reference to the trajectories of the marked fluid elements. We focus our analysis on a rigid sphere of radius $a$ that is steadily towed through an unbounded viscous fluid by an external force. The initial profile of the marked fluid is taken to be a disk of finite height $h$, and $h$ is furthermore assumed to be much larger than $a$. A two-term asymptotic expansion of $D$ for $h/a \to \infty$ is computed for $\mathrm{Re} = 0$ and compared to the analogous result for inviscid flow in order to illustrate the fundamental differences between these two cases. Next, a leading-order approximation to $D$ for a sphere translating at small Re is computed using Oseen's approximation to the flow. These results are extended to $\mathrm{Re} \geqslant O(1)$ by taking advantage of the fact that, at distances greatly exceeding its radius, the flow around a sphere is described by the point force solution to Oseen's equations. Therefore, it is found universally that $D$ diverges as the distance traveled by the sphere becomes large at finite Re. However, the exact nature of this divergence critically depends upon the ratio of the distance traveled by the sphere to the radius of the initially marked disk of fluid ($h$).

DOI: 10.1103/PhysRevFluids.2.064101

## I. INTRODUCTION

*Drift* refers to the permanent displacement of fluid elements disturbed by the passage of a body through a bulk fluid. Advection due to drift is an important mechanism of heat and mass transport enhancement in a variety of natural and industrial processes. For example, heat transfer in pool boiling is greatly enhanced by the drift induced by rising bubbles that nucleate at the source of heat [1]. In gas-fluidized beds, the movement of gas voids through a particulate medium is analogous to the motion of an inviscid bubble through a fluid, and the resulting drift is an important source of mixing [2]. Drift is also relevant to froth flotation, a process used in the mining industry in which rising air bubbles separate minerals from an aqueous slurry. Water carried upward with the bubbles induces recirculation within froth flotation columns, negatively impacting performance [3]. Yet another example is provided by the bubble aeration systems of bioreactors, which are critical to reactor performance. Enhanced mass transport due to the bubbling is important to reducing biofouling and maintaining desirable oxygen and carbon dioxide levels [4,5].

Recent interest in drift was sparked by the suggestion of Katija and Dabiri [6] that drift is an important mechanism in biogenic ocean mixing. Drift is viscosity enhanced, meaning that the total volume of fluid displaced (relative to the volume of the body) increases as viscous forces become

*akhair@andrew.cmu.edu

 

increasingly important (i.e., with decreasing Reynolds number). This lends support to the possibility that small, millimeter-scale, swimming organisms, such as krill or copepods, which make up the dominant fraction of the oceanic animal biomass, may induce large-scale mixing [7]. Their work prompted further theoretical and experimental investigations into the drift induced by swimmers at small and intermediate Reynolds numbers and its possible impact on ocean stirring [8–11]. Drift has also been investigated in the context of vortex motion [12,13], recirculatory wakes behind bluff bodies [14,15], multibody problems [16,17], stratified fluids [18], and protein transport in cellular membranes [19].

Classic investigations of the trajectories traced out by fluid elements as a result of a passing body date back to Rankine [20] and Maxwell [21], who considered a circular cylinder steadily translating through an unbounded inviscid fluid. Fluid elements follow along streamlines in the reference frame that moves with the cylinder. However, a simple Galilean change of reference frame into that in which the fluid far from the cylinder is at rest reveals that, in this frame, fluid elements follow complex, looping paths. Moreover, they are permanently displaced some distance forward after the body is made to travel a long distance. This phenomenon was further investigated by Darwin [22], who referred to it as *drift*.

In order to conveniently quantify the total volume of fluid displaced or entrained by a translating body, Darwin introduced the concept of the drift volume. The drift volume $D$ is defined as the volume enclosed between the initial and final profiles of a marked (as in with dye) material surface, as the body translates from an infinite distance behind to an infinite distance in front of the plane on which the fluid was initially marked. The initial material plane is infinite in extent and perpendicular to the body's path of motion. Thus, $D$ may be interpreted as the volume of fluid eventually entrained by the passing body. Darwin's analysis of the drift volume in inviscid flow revealed the remarkable result that $D = m_a/\varrho$, where $m_a$ is the added mass of the body and $\varrho$ is the fluid density. This relation is often referred to as Darwin's theorem or Darwin's proposition. Further proofs of Darwin's theorem were put forth by Yih [23]. The result of the theorem is unexpected in at least two respects. First, the sphere must displace a volume of fluid equal to its own volume as it translates, suggesting there should be a net reflux of fluid opposite to the direction of travel. However, the positive sign of $D$ indicates a net *forward* flux instead. Second, it is not immediately obvious why $D$ should be so closely tied to $m_a$. The added mass describes the apparent additional mass of an accelerating body in a fluid due to the increasing kinetic energy of the surrounding fluid. The drift volume, however, has no inherent association with fluid acceleration. We will not discuss this further here, but some physical insight into this surprising relationship is provided by Yih [23,24].

However, caution is necessary in the application of Darwin's theorem, causing some debate about whether it is more appropriately referred to as a proposition [24–26]. As pointed out by Darwin himself, the procurement of the relation $D = m_a/\varrho$ is dependent upon the ordering of nested improper integrals involved in computing $D$, which are taken over all space. Evaluating $D$ amounts to evaluating the total momentum of the fluid (divided by $\varrho$), which is itself indeterminate [25]. The physical origins of this indeterminacy were elucidated by Eames *et al.* [26], who extended Darwin's concept by introducing the *partial* drift volume $D_p(x_0,h)$, which is a determinant quantity. In this case, the body is placed at an initial position $x_0$ relative to the marked plane, which is a disk of finite height $h$. Assuming that $h$ far exceeds the dimensions of the body ($h \to \infty$), one expects to recover $D_p(x_0,h) \to m_a/\varrho$ as the distance of the body from the marked plane is made infinite ($x_0 \to -\infty$). However, this is only true if $x_0/h \to -\infty$. In fact, $D_p$ depends critically on the ratio $x_0/h$, although it is always finite and comparable in magnitude to the volume of the body $V_b$. For instance, if $x_0/h \to 0^-$, then $D_p(x_0,h) \to -V_b$. In this case, the drift volume represents a net backward reflux of fluid, itself equal in magnitude to the volume of the body.

Another limitation of Darwin's theorem is that it formally applies only to inviscid fluids. Let $\mathrm{Re} \equiv 2\varrho U l_c/\mu$ be the Reynolds number, where $U$ is the speed of the body, $\mu$ is the fluid viscosity, and $l_c$ is the characteristic length of the body. Darwin's theorem is of practical value only in cases where Re is sufficiently large for the effects of viscosity to be negligible. In such scenarios, where the majority flow is approximately irrotational, experimental results for $D$ indeed exhibit reasonable

agreement with the prediction $D = m_a/\varrho$ [12,13,27,28]. However, any body moving through an unbounded fluid by the action of an external force at finite Re carries with it a viscous wake of nonzero vorticity. The velocity disturbance in the wake decays as $v \sim 1/r$, where $v$ is the magnitude of the velocity disturbance and $r$ is the radial distance from the body [29]. This slow decay suggests that the displacement of any fluid element entrained by the wake diverges logarithmically as the body translates an infinite distance, and thus $D$ is unbounded [8]. Disagreement between Darwin's theorem and experiments on rising bubbles at $\mathrm{Re} \approx 100$ can be attributed to this fact [30].

The nature of the drift volume in viscous flows has not been studied to the same extent as in the inviscid case, although there are some theoretical predictions for Stokes flow ($\mathrm{Re} = 0$). Eames *et al.* [31] computed a leading-order approximation to $D_p$ induced by a translating spherical droplet of radius $a$ in Stokes flow as $h/a \to \infty$, which is found to diverge with time $t$ (i.e., as the distance traveled by the droplet, $Ut$, becomes large). This is due to the slow velocity decay of the Stokeslet (force monopole) contribution to the flow, which has $v \sim 1/r$ everywhere. However, it is also found that if the fluid is bounded by a wall, $D_p$ is instead convergent because $v$ decays faster than $1/r$ in the far field, and hence marked fluid elements translate only a finite distance as $t \to \infty$. For a wall parallel to the travel direction, $v \sim 1/r^2$, and for a perpendicular wall, $v \sim 1/r^3$. The drift volume induced by a disk translating through a two-dimensional porous medium has also been considered [19]. Here, $D$ and $D_p$ are also bounded because $v \sim 1/r^2$ at distances greater than the Brinkman screening length, upon which $D$ is shown to be quadratically dependent.

Additionally, the drift volume induced by a spherical microswimmer (a "squirmer") of radius $a$ at $\mathrm{Re} = 0$ has been investigated by Leshansky and Pismen [9] and Pushkin *et al.* [10]. The flow generated by such a swimmer can be described by a combination of a stresslet (symmetric force dipole) contribution and a potential dipole contribution. Whether the swimmer generates thrust from the front or rear (i.e., is a "pusher" or "puller," respectively) is dictated by the sign of the stresslet, while the potential dipole can be interpreted as an irrotational treading of the fluid past the swimmer. There is no Stokeslet contribution to the flow because the swimmer is assumed to be free of external forces and translating steadily. Thus, the stresslet, which has $v \sim 1/r^2$, makes the dominant contribution to the far-field flow. However, its fore-aft mirror symmetric velocity distribution dictates that its net contribution to $D$ cancels as the swimmer translates from far behind to far ahead of the initially marked fluid plane. The potential dipole component of the flow ($v \sim 1/r^3$) is left to determine $D$, and it is found that $D = V_b/2 = 2\pi a^3/3$. The same result is coincidentally recovered for a sphere moving through an inviscid fluid.

The drift volume induced by a body moving through a viscous fluid at finite Re has yet to be quantified in detail, and doing so is the central goal of this article. Our goal is of fundamental fluid mechanical interest and has practical value, since past [30] and recent [11,18] experiments have examined drift at finite Re, for which there is a lack of existing theoretical predictions. We develop a general and intuitive framework for computing the drift volume by interpreting the drift volume as the time-integrated flux through a stream tube. For simplicity, we limit ourselves to the problem of the drift volume induced by a rigid sphere of radius $a$ translating through an unbounded fluid at a steady speed $U$ as a function of Re. Further, we restrict ourselves to the case where the radius of the initially marked fluid disk $h$ is much larger than $a$, since this is typically the case of greatest interest, and because it allows us to make asymptotic approximations to $D_p$. Considering this simplified problem will contribute to a better understanding of drift in more complex systems, such as that due to bubbling in reactor columns and swimming organisms in the world's lakes and oceans. Moreover, the methodology we develop may be readily applied to more complicated problems, including drift in stratified fluids or in bounded fluid domains.

It has been previously suggested that the partial drift volume at finite Re is tied to the volumetric flux $Q$ through the viscous wake downstream of the body. This flux is constant at distances far downstream and is related to the drag $F$ on the body as $Q = F/\varrho U$ [29]. Therefore, one may surmise that $D_p$ diverges linearly with time as $t \to \infty$, at a rate that is proportional to $F$ [9,26]. However, this argument assumes that $h$ is always large compared to the traverse size of the wake, which also diverges with the downstream distance. It also neglects the sourcelike flow emanating

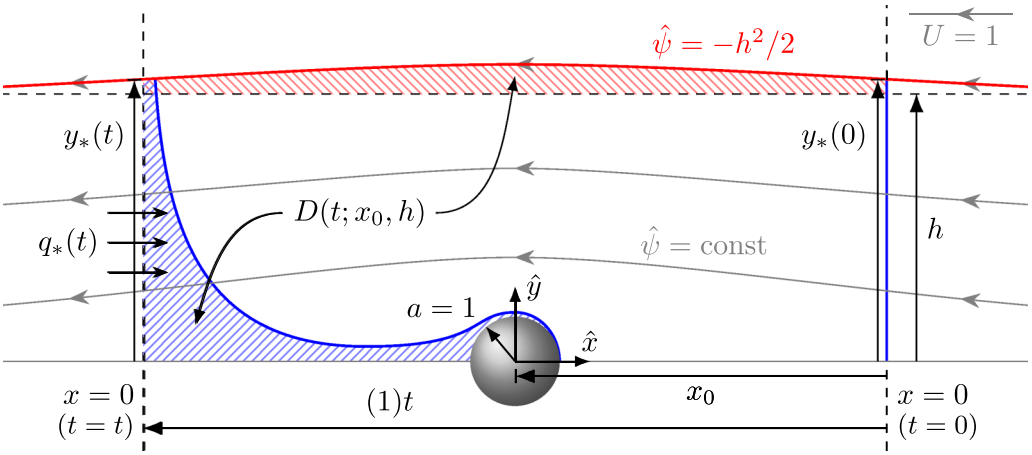


FIG. 1. An illustration of the drift volume in the comoving frame, in which a uniform flow approaches a sphere of unit radius from the right at unit velocity. At $t = 0$, the fluid is marked at $x = 0$ for $y < y_*(0)$, as indicated by the solid line to the right of the sphere. The sphere is at an initial distance $x_0$ from the $x = 0$ plane. At time $t > 0$, the sphere translates a distance of $(1)t$ toward and eventually past $x = 0$, causing the marked fluid to deform. The volume swept out by the marked fluid at time $t$ is indicated by the shaded area to the left of the sphere and is defined to be the drift volume, $D(t; x_0, h)$. The fluid volume between $y = h$ and the streamline $\hat{\psi} = -h^2/2$, represented by the shaded area above the sphere, is also equal to $D$. The rate at which $D$ increases with $t$ is equal to the volumetric flux, $q_*(t)$, through $x = 0$ for $y < y_*(t)$.

from the sphere that compensates the flux through the wake. As we will show, the behavior of $D_p$ at finite Re is more complex than has been previously suggested. Moreover, although $D_p$ always diverges as $t \to \infty$, the nature of this divergence depends critically on assumptions regarding the ratio of the total distance traversed by the sphere to the extent of the marked plane, as these quantities are made unboundedly large. This behavior is analogous to the conditional nature of Darwin's theorem, $D = m_a/\varrho$, in inviscid flow.

In Sec. II, we generalize the partial drift volume concept to finite travel times by introducing a definition that we show to have two distinct geometrical interpretations. Another way of doing so is given by Camassa *et al.* [32], but their argument requires $v$ to decay faster than $1/r$ in the far field. The flux argument that we develop has no such limitation, and thus we may readily apply it to (unbounded) Stokes flows and flows at finite Re (where the velocity in the wake decays as $1/r$). We first review the classic inviscid flow problem in Sec. III, where we validate our method of computing $D_p(t)$ against previous analytical results. From there, we consider Stokes flow in Sec. IV, where a two-term asymptotic expansion for $D_p(t)$ is derived for $h/a \gg 1$. In Sec. V, we obtain an approximation to $D_p$ at small Re using Oseen's approximation of the flow. Finally, we consider the drift volume associated with the point force solution to Oseen's equations, which gives a general estimate of $D_p$ for a body translating in steady, laminar flow. A brief discussion of the overall results is presented in Sec. VII, which are finally summarized in Sec. VIII. For brevity, we will henceforth use the term *drift volume* to refer to the partial drift volume $D_p$ as a general function of $t$, $x_0$, and $h$, and we will omit the subscript $p$.

## II. DEFINITION OF THE DRIFT VOLUME

Consider an impermeable sphere of radius $a$ translating steadily through an unbounded fluid at speed $U$ in the positive direction along the $x$ axis (Fig. 1). We will normalize distance by $a$ and time $t$ by $a/U$, and all quantities defined henceforth will be dimensionless unless stated otherwise. Let the $y$ coordinate measure the distance from the $x$ axis, such that $(x, y)$ specifies a position in a

cylindrical coordinate system in which the fluid far from the sphere is at rest (the fixed frame). The flow is assumed to be axisymmetric about the $x$ axis so that there is no dependence on the azimuthal angle. At $t = 0$, let the initial position of the sphere be $(x_0,0)$. Also, in the frame that is comoving with the sphere, let $\hat{x}$ and $\hat{y}$ be the coordinates centered on the sphere such that $\hat{x} = x - (x_0 + t)$ and $\hat{y} = y$. The flow is assumed to be steady in this frame, and thus it may be described by a stream function $\hat{\psi}(\hat{x},\hat{y})$, which is normalized by $Ua^2$ and tends toward $-\hat{y}^2/2$ in the far field. At $t = 0$, the fluid on the $x = 0$ plane is marked (as in with dye) for $y < y_*(0)$, where the point $(0, y_*(t))$ is the intersection of the $x = 0$ plane with the streamline, $\hat{\psi} = -h^2/2$, that approaches $y = h$ as $x \to \pm\infty$. Driven by the motion of the sphere, the marked fluid deforms as time progresses from $t = 0$. Now, consider the fluid enclosed by the $x = 0$ plane, the marked material surface of fluid, and the fluid lying on $\hat{\psi} = -h^2/2$, which also constitutes a material surface. Let the (dimensionless) drift volume $D = D(t; x_0,h)$ be defined as the volume of fluid, normalized by $a^3$, contained within this region at a particular time $t > 0$, which is depicted as the shaded area trailing the sphere in Fig. 1. The partial drift volume, as defined by Eames *et al.* [26], is reproduced in the limit $t \to \infty$, as the streamlines become flat at an infinite downstream distance from the sphere. Darwin's drift volume is also reproduced upon letting $x_0 \to -\infty$, $t \to \infty$, and $h \to \infty$ (although the ordering of these limits requires care, as we will discuss later).

This definition of the drift volume is particularly useful because it reveals that $D$ may be interpreted as the time-integrated flux through a kinematic surface within the fluid domain. Let $A = A(t)$ represent such a surface lying on $x = 0$ for $y < y_*(t)$ (with area $\pi y_*^2$), and let $q_* = q_*(t)$ represent the volumetric flux through $A$. All boundaries of the region defining the drift volume are material surfaces except $A$, including the surface of the sphere itself. Therefore, a material balance dictates that $D = \int_0^t q_*(t)\,dt$. Our flux interpretation of $D$ is similar to that of Benjamin [25]; it only differs in that we bound $A$ by a streamline (or, more accurately, a stream tube), rather than by an arbitrary time-independent circle of constant radius ($>a$). Our modification ensures that $D(t \to \infty; x_0,h)$ is consistent with the partial drift volume considered by Eames *et al.* [26].

Let $\psi(x,y,t) = \hat{\psi}(\hat{x},\hat{y}) + \hat{y}^2/2$ represent the instantaneous stream function of the flow in the fixed frame. The difference in $\psi$ between any two points is equivalent to ($2\pi$ times) the flux through any instantaneous axisymmetric surface connecting those points. Thus, we may evaluate the flux through $A(t)$ as $q_*(t) = 2\pi[\psi_*(t) - \psi_b(t)]$, where $\psi_*(t) = \psi(0, y_*(t),t)$, and $\psi_b(t)$ is $\psi$ evaluated at the intersection of the $x = 0$ plane with the sphere's surface. When there is no intersection, $\psi_b = 0$. Integrating $q_*(t)$ over time yields

$$D = 2\pi \int_0^t [\psi_*(t') - \psi_b(t')]dt' = 2\pi \int_0^t \psi_*(t')dt' - [\bar{V}_b(t) - \bar{V}_b(0)], \tag{1}$$

where $\bar{V}_b(t)$ is the volume of the sphere (normalized by $a^3$) that has passed through $x = 0$ at time $t$. The second equality in (1) holds as long as the sphere is impermeable.

There is a second possible interpretation of the drift volume. An implicit relation between $\psi_*$ and $y_*$ is given by

$$\psi_* = \tfrac{1}{2}y_*^2 - \tfrac{1}{2}h^2. \tag{2}$$

Inserting (2) into (1) gives

$$D = \pi \int_0^t y_*^2(t')dt' - \pi h^2 t - [\bar{V}_b(t) - \bar{V}_b(0)]. \tag{3}$$

The first two terms on the right-hand side of (3) evidently describe a volume of revolution about the $x$ axis that is bounded above by $\hat{\psi} = -h^2/2$ and below by $y = h$, as highlighted in Fig. 1. The equivalence of $D$ to the volume between this streamline and its unperturbed (free-stream) position can be realized by a direct geometrical argument [23] that has been utilized by others [9,10,31]. However, the flux interpretation that we outlined here has not been previously emphasized, and thus it is worth pointing out the mathematical equivalence between these two interpretations of $D$.

Solving (2) for $\psi_*$ as an explicit function of time in the interest of evaluating (1) is complicated by the fact that $\psi(x,y,t)$ is generally a nonlinear function of space and time. To ameliorate this issue, and because we are primarily concerned with the motion of the entirety of the bulk fluid as the sphere translates, we will restrict our attention to the case where $h \gg 1$, i.e., where the radius of the marked disk of fluid is large compared to that of the sphere. Then, $y_*/h \sim 1$ for all $t$ since the departure from the uniform stream is small far from the sphere. In this case, it is convenient to define $\tau = (x_0 + t)/h$ and $\rho = y_*/h$. We may rearrange and express (2) in terms of these variables as

$$\rho^2 = 1 + \frac{2\psi_*}{h^2}. \tag{4}$$

The integral for the drift volume from (1) then becomes

$$D = 2\pi h \int_{\tau_0}^{\tau} \psi_*(\tau')d\tau' - [\bar{V}_b(\tau) - \bar{V}_b(\tau_0)], \tag{5}$$

where $\tau_0 = \tau|_{t=0} = x_0/h$. For brevity, we will make use of the function $\Delta(\tau;h) = D(\tau,\tau_0 = 0,h)$, from which $D(\tau) = \Delta(\tau) - \Delta(\tau_0)$. We may interpret $\Delta(\tau)$ as the downstream drift volume, occurring after the center of the sphere has crossed $x = 0$. Conversely, $-\Delta(\tau_0)$ is the upstream drift volume occurring before the center of the sphere crosses $x = 0$.

## III. INVISCID FLOW

The flow due to a sphere passing through an inviscid fluid is described by a potential dipole at the center of the sphere. Thus, the instantaneous stream function in the fixed frame evaluated at $(0, y_*(t))$ is given by

$$\psi_* = \frac{\rho^2}{2h(\tau^2 + \rho^2)^{3/2}}. \tag{6}$$

Inserting (6) into (4) yields a nonlinear equation for $\rho(\tau)$,

$$\rho^2 = 1 + \frac{\rho^2}{h^3(\tau^2 + \rho^2)^{3/2}}. \tag{7}$$

For $h \gg 1$, (7) makes apparent that there is only a very small, $O(1/h^3)$, deflection from the free-stream flow. This suggests that we may make a leading-order approximation to $D$ by setting $\rho = 1$ in (6). Hence, from (5), an approximation to the drift volume is

$$D \sim D_0 = 2\pi \int_{\tau_0}^{\tau} \frac{ds}{s^2 + 1} - [\bar{V}_b(\tau) - \bar{V}_b(\tau_0)]. \tag{8}$$

Evaluating (8) gives

$$\Delta \sim \Delta_0 = \frac{\pi\tau}{\sqrt{\tau^2 + 1}} - \bar{V}_b(\tau). \tag{9}$$

This approximation to the drift volume is essentially the same as that considered by Benjamin [25]. We may physically interpret $D_0$ as the volume of fluid through a disk of radius $h$ at $x = 0$, since we have effectively neglected the deflection of streamlines far from the sphere. Interestingly, the drift volume only depends on $x_0$, $h$, and $t$ through $\tau$ (and $\tau_0$) at this level of approximation. The fact that $h$ does not appear in (9) indicates that $D$ converges to an $O(1)$ value as the height of the marked plane is made large. Also, we observe that $\Delta_0(\tau) = -\Delta_0(\tau_0)$ due to the fore-aft symmetry of the flow.

If an unbounded marked plane ($h \to \infty$) is considered, corresponding to Darwin's original calculation, then the error incurred by setting $\rho = 1$ in (6) approaches zero, and $D \to D_0$. However, this places no restriction on the values of $x_0$ or $t$, which may be unboundedly large. The ratios $\tau$ and $\tau_0$ are in this case indeterminate and must be specified for $D(\tau)$ to be well defined [25,26]. In order

to recover the equivalence of the drift volume (multiplied by the fluid density) to the added mass, as originally done by Darwin, the distance traveled by the sphere must be assumed to be infinitely large compared to the marked plane. This corresponds to letting $\tau_0 \to -\infty$ and $\tau \to \infty$ in (9). From this, we obtain the expected result that $D = 2\pi - V_b = 2\pi/3$, where $V_b$ is the total (dimensionless) volume of the sphere, $4\pi/3$. If instead the path traversed by the sphere is infinitesimal compared to $h$ (although large compared to $a$), then $\tau \to 0$ for all $t$. The first term in (9) consequently vanishes, and $D = -V_b = -4\pi/3$ (a result that was also obtained by Darwin). Finally, $\tau$ or $\tau_0$ may be taken as finite, in which case intermediate values of $D$ are obtained. However, despite its conditional nature, $D$ is always comparable in magnitude to $V_b$.

We may obtain corrections to $D(\tau;\tau_0,h)$ for large (but finite) $h$ by an asymptotic expansion in terms of the small parameter $\varepsilon = 1/h$. In this manner, the effect of the small deflection of the streamline $\hat{\psi} = -h^2/2$ may be accounted for. Equation (6) suggests an expansion for $\rho(\tau;\varepsilon)$ of the form $\rho^2 = 1 + \varepsilon^3\rho_3^2(\tau) + \varepsilon^6\rho_6^2(\tau) + O(\varepsilon^9)$. After substituting this series into (7) and expanding each term as a Taylor series about $\varepsilon = 0$, matching like powers of $\varepsilon$ gives

$$\rho^2 = 1 + \frac{\varepsilon^3}{u^3} + \varepsilon^6\left(\frac{1}{u^6} - \frac{3}{2u^8}\right) + O(\varepsilon^9), \tag{10}$$

where $u = \sqrt{\tau^2+1}$. We may directly obtain a corresponding expansion for $\psi_*$ using (4); namely,

$$\psi_* = \frac{\varepsilon}{2u^3} + \varepsilon^4\left(\frac{1}{2u^6} - \frac{3}{4u^8}\right) + O(\varepsilon^7). \tag{11}$$

This may be substituted into (5) and integrated by making the hyperbolic substitution $\tau = \sinh\theta$ and applying the reduction formula $(n-1)\int \operatorname{sech}^n\theta d\theta = \operatorname{sech}^{n-2}\theta\tanh\theta + (n-2)\int \operatorname{sech}^{n-2}\theta d\theta$. The expansion $\Delta(\tau;\varepsilon) = \Delta_0(\tau) + \varepsilon^3\Delta_3(\tau) + O(\varepsilon^6)$ is thereby obtained, where

$$\Delta_3(\tau) = -\frac{\pi}{32}\left[3\tan^{-1}\tau + \frac{3\tau}{(\tau^2+1)} + \frac{2\tau}{(\tau^2+1)^2} + \frac{8\tau}{(\tau^2+1)^3}\right]. \tag{12}$$

From (12), we observe that $\Delta_3$ decreases (very nearly) monotonically with $\tau$ (the last bracketed term produces weak nonmonotonicity). Therefore, $\Delta_3$ represents a reflux of fluid opposite to the direction of travel. Taking the limit of $D$ as $\tau \to \infty$ and $\tau_0 \to -\infty$, all of the bracketed terms in (12) vanish except for the monotonic $\tan^{-1}\tau$ term. Thus, $D = 2\pi/3 - 3\pi^2\varepsilon^3/32 + O(\varepsilon^6)$. The results for $D(\tau;\tau_0,h)$ given by (9) and (12) are plotted in Fig. 2(a). They are consistent with other asymptotic analyses of the drift volume in inviscid flow [26,32] and serve to validate our method for computing $D$.

## IV. STOKES FLOW

Repeating the analysis for Stokes flow ($\mathrm{Re} = 0$) past a rigid spherical particle with a no-slip surface is straightforward; the procedure requires little modification from the inviscid flow case considered in Sec. III. Here, the stream function at $(0, y_*(t))$ is

$$\psi_* = \frac{3h}{4}\frac{\rho^2}{(\tau^2+\rho^2)^{1/2}} - \frac{1}{4h}\frac{\rho^2}{(\tau^2+\rho^2)^{3/2}}. \tag{13}$$

The large $O(h)$ term in (13) is contributed by the Stokeslet, which dominates the flow far from the sphere. The much weaker $O(1/h)$ term is due to a potential dipole contribution to the flow, required to satisfy the no-slip condition at the sphere surface [it is of the same form that appears in (6)].

Inserting (13) into (4) gives

$$\rho^2 = 1 + \frac{3}{2h}\frac{\rho^2}{(\tau^2+\rho^2)^{1/2}} - \frac{1}{2h^3}\frac{\rho^2}{(\tau^2+\rho^2)^{3/2}}. \tag{14}$$

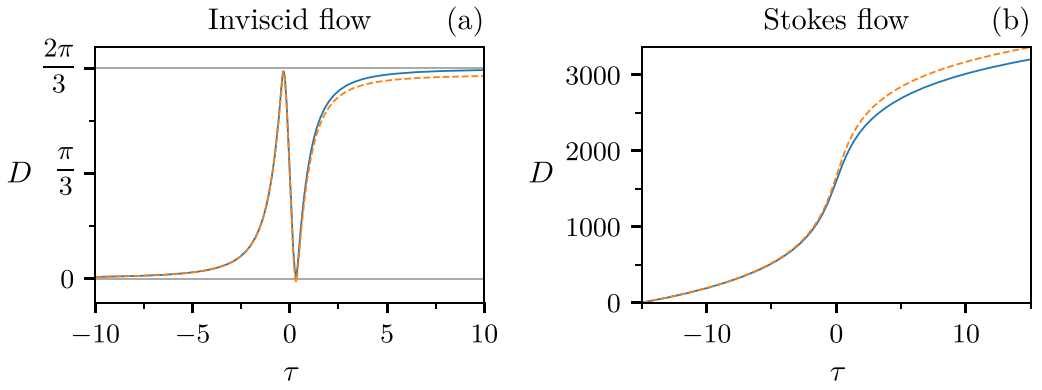


FIG. 2. The drift volume $D$ (normalized by $a^3$) for a rigid sphere in inviscid flow (a) and in Stokes flow (b). The solid lines represent the leading-order approximations to $D$ from (9) and (15), respectively, and the dashed lines represent the asymptotic corrections given by (12) and (16), respectively. In panel (a), $h = 2.5$ and $\tau_0 \to -\infty$. The sharp drop in $D$ at $\tau = 0$ is the result of the sphere displacing fluid as it passes through the $x = 0$ plane. Darwin's result that $D = 2\pi/3$ is approached as $\tau$ becomes large. In panel (b), we have taken $h = 10$ and $\tau_0 = 15$. Note that the magnitude of $D$ in Stokes flow is orders of magnitude greater than that in inviscid flow.

Compared to the inviscid case, where the deflection from the uniform stream is only $O(h^{-3})$ [see (7)], (14) shows a more significant $O(h^{-1})$ deflection. Nonetheless, the flow is approximately uniform far from the sphere, and a leading-order approximation to $D(\tau;\tau_0,h)$ may again be obtained by neglecting the vertical deflection of streamlines for $h \gg 1$. Setting $\rho = 1$ in (13) and evaluating the resulting integral in (5) yields

$$\Delta \sim \Delta_0 = \frac{3\pi}{2} h^2 \sinh^{-1}\tau, \tag{15}$$

which we plot with $h = 10$ in Fig. 2(b). Note that Eames *et al.* [31] obtain a similar result, which can be verified to be in agreement with (15) after rewriting $\tau$ in terms of the angle $\theta$, with reference to the center of the sphere, subtended by the $x$ axis and the point $(0, y_*)$ at time $t$. Namely, it can be shown that $\sinh^{-1}\tau = \sinh^{-1}(-\cot\theta) = \ln(\tan\frac{1}{2}\theta)$.

The sole term in (15) is contributed by the Stokeslet and is $O(h^2)$. Other contributions to $\Delta(\tau;h)$ coming from the second term in (13) and $\bar{V}_b(\tau)$ are only $O(1)$. Hence, they are omitted from (15), which, as we will formally show below, has $O(h)$ error. From this leading-order result, we find that $\Delta(\tau) = -\Delta(\tau_0)$, which is due to the fore-aft flow symmetry and is a property that is shared with the inviscid flow case. However, we also observe that $D$ diverges linearly with the area, projected onto a plane perpendicular to the $x$ axis, of the marked fluid as $\tau \to \infty$, $\pi h^2$, and hence quadratically with $h$. It also diverges logarithmically with $\tau$ as $\tau \to \infty$ (since $\sinh^{-1}\tau \sim \ln\tau$ for $\tau \gg 1$), and there is a similar divergence as $\tau_0 \to -\infty$ (as the initial distance of the sphere from the marked fluid is made large). This behavior contrasts drastically with that found for inviscid flow, where $D$ converges to an $O(1)$ value as $h \to \infty$ and $t \to \infty$. The divergent nature of $D$ in Stokes flow can be attributed to the slow $1/r$ decay of the velocity disturbance. The total horizontal displacement of marked fluid elements $X(t)$ (in the fixed frame) scales as $X \sim \int^t dt/t = \ln t$ as $t \to \infty$. This can be compared with the far weaker $v \sim 1/r^3$ decay in inviscid flow, which leads to a bounded fluid displacement.

Recall the indeterminate nature of $D(t;x_0,h)$ in inviscid flow, which is due to assumptions made regarding $\tau$ as $x_0 \to \infty$, $t \to \infty$, and $h \to \infty$. The same issue must be addressed for Stokes flow. If we allow that $\tau = (x_0 + t)/h \gg 1$, so that the path of travel far exceeds $h$, then $D$ diverges logarithmically with $t$ according to (15). However, if the path of travel is not large compared to $h$, such that $\tau = (x_0 + t)/h \ll 1$ for all $t$, then (13) gives $\psi_* \sim 3h/4$, which is interestingly independent of $\tau$. This implies a constant volumetric flux through all planes perpendicular to the $x$ axis, and

hence that $D \sim 3\pi ht/2$. Thus, $D$ diverges linearly, rather than logarithmically, with $t$ at long times in this case. This behavior is also contained within (15), which can be verified by evaluating the Taylor expansion of $\Delta_0(\tau; h)$ about $\tau = 0$ to leading order in $\tau$.

Corrections to $\Delta_0$ for small but finite $\varepsilon = 1/h$ may be obtained in the same manner as for the inviscid flow case, with the exception that $\rho^2$ must be expanded in powers of $\varepsilon$ instead of $\varepsilon^3$, as indicated by the presence of an $O(\varepsilon)$ term in (14). Performing the expansion yields

$$\Delta = \frac{3\pi}{2}h^2 \sinh^{-1}\tau + h\left(\frac{27\pi}{16}\tan^{-1}\tau - \frac{9\pi\tau}{16(\tau^2+1)}\right) + O(1). \tag{16}$$

The second term in (16) represents an $O(h)$ correction to the leading-order result, $\Delta_0$, from (15). It increases monotonically, therefore representing a net drift of fluid in the same direction as the sphere, rather than a reflux, as was found for the analogous correction in inviscid flow (12). This may be attributed to the fact that, in Stokes flow, the velocity in the fixed frame is everywhere in the direction of travel, and the corresponding streamlines are therefore open. In inviscid flow, the streamlines are closed in loops, and the flow moves opposite to the direction of travel for $\hat{y}^2 > 2\hat{x}^2$. Note that the correction to $\Delta(\tau; h)$ in (16) is more significant compared to that for inviscid flow in the sense that its magnitude differs from the leading-order term by a factor of $1/h$, as compared to $1/h^3$.

## V. SMALL REYNOLDS NUMBERS

To quantify the effect of inertia on the drift volume, we first consider Oseen's approximation to the flow for $\mathrm{Re} \ll 1$ [33]. Here, we define the Reynolds number as $\mathrm{Re} = 2\varrho Ua/\mu$. In this approximation, the stream function for the flow produced by a steadily translating rigid sphere with a no-slip surface evaluated at $(0, y_*(t))$ is

$$\psi_* = \frac{3}{\mathrm{Re}}\left(1 + \frac{\tau}{\sqrt{\tau^2+\rho^2}}\right)\left\{1 - \exp\left[-\frac{\mathrm{Re}h}{4}(\sqrt{\tau^2+\rho^2} - \tau)\right]\right\} - \frac{1}{4h}\frac{\tau^2}{(\tau^2+\rho^2)^{3/2}}. \tag{17}$$

We anticipate that the Oseenlet (i.e., the solution to Oseen's equations for a point force), represented by the first term in (17), will make the dominant contribution to $D$. Hence, the $O(1)$ contribution of the remaining potential dipole term is neglected, and the $\bar{V}_b(\tau)$ contribution from (5) is omitted for the same reason. Finally, the deflection of the $\hat{\psi} = -h^2/2$ streamline, which we expect to have a relatively small effect on $D$, is neglected by setting $\rho = 1$. With these approximations, (17) in (5) gives

$$D_0 = \frac{6\pi h}{\mathrm{Re}}\int_{\tau_0}^{\tau}\left(\frac{s}{\sqrt{s^2+1}} + 1\right)\left\{1 - \exp\left[-\frac{\mathrm{Re}h}{4}(\sqrt{s^2+1} - s)\right]\right\}ds, \tag{18}$$

which represents a first approximation to $D$ for $h \gg 1$ and $\mathrm{Re} \ll 1$. By making the substitution $u(\tau) = \sqrt{\tau^2+1} - \tau$, (18) may be simplified to

$$D_0 = \frac{6\pi h^2}{\mathrm{Re}_h}\int_{u(\tau_0)}^{u(\tau)}\left[1 - \exp\left(-\frac{1}{4}\mathrm{Re}_h u\right)\right]d\left(\frac{1}{u}\right), \tag{19}$$

where $\mathrm{Re}_h = \mathrm{Re}h$ is the Reynolds number based on $h$. Evaluating (19) in terms of the exponential integral, $E_1(z) \equiv \int_z^\infty \exp(-x)/x\,dx$, gives

$$\Delta_0(u) = \frac{3\pi h^2}{2}\left[\frac{1 - \exp\left(-\frac{1}{4}\mathrm{Re}_h u\right)}{\frac{1}{4}\mathrm{Re}_h u} + E_1\left(\frac{1}{4}\mathrm{Re}_h u\right)\right] - C, \tag{20}$$

where

$$C = \frac{3\pi h^2}{2}\left[\frac{1 - \exp\left(-\frac{1}{4}\mathrm{Re}_h\right)}{\frac{1}{4}\mathrm{Re}_h} + E_1\left(\frac{1}{4}\mathrm{Re}_h\right)\right].$$

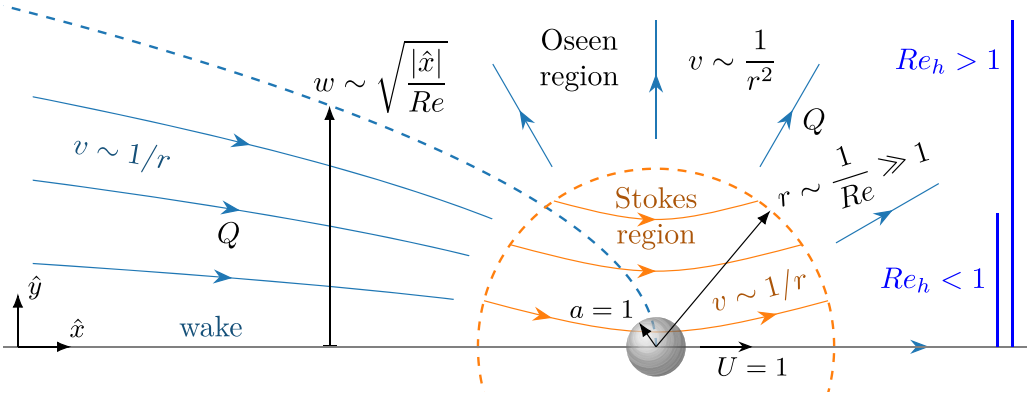


FIG. 3. A sketch of the flow pattern produced by a rigid sphere translating steadily at Re $\ll 1$. Here, $r$ is the radial distance from the sphere, $v$ is the magnitude of the velocity disturbance, and $w$ is the transverse dimension of the parabolic wake. There is a constant volumetric flux $Q$ through the wake that is compensated by the source-like flow in the remainder of the Oseen region. The solid vertical lines to the right of the sphere represent the vertical extent of the initially marked fluid.

The magnitude of $\mathrm{Re}_h$, which (20) suggests is centrally important to the behavior of $D_0(\tau)$, quantifies how much the motion of the marked fluid is influenced by inertial versus viscous forces. It may be interpreted as the ratio of the height of the marked fluid $h$ to the distance from the sphere, $r \sim 1/\mathrm{Re} \gg 1$, at which inertial and viscous forces balance. The general pattern of flow around the sphere is illustrated in Fig. 3. Viscous forces dominate where $r \ll 1/\mathrm{Re}$, in the Stokes region, but are balanced by inertial forces at $r = O(1/\mathrm{Re})$, in the Oseen region. At distances far into the Oseen region, where $r \gg 1/\mathrm{Re}$, inertia dominates, and the majority of the flow is irrotational with a sourcelike character. However, the Oseen region features a parabolic wake downstream of the sphere where viscous forces remain relevant, even far outside of the Stokes region. The width of the wake as a function of the distance downstream of the sphere is described by $w \sim \sqrt{-\hat{x}/\mathrm{Re}}$, and hence $w|_{x=0} \sim h\sqrt{\tau/\mathrm{Re}_h}$. It follows that the size of the wake is comparable to the height of the marked fluid ($w \sim h$) when $\tau \sim \mathrm{Re}_h$. Therefore, $\mathrm{Re}_h$ has the second interpretation of being the dimensionless distance downstream of the sphere beyond which the majority of the marked fluid becomes entrained by the viscous wake.

The result from (20) is shown in Fig. 4, where we have normalized $D_0$ by $h^2$ in order to collapse (20) to a single curve for each value of $\mathrm{Re}_h$. Here, $\mathrm{Re}_h = 0$ corresponds to the leading-order

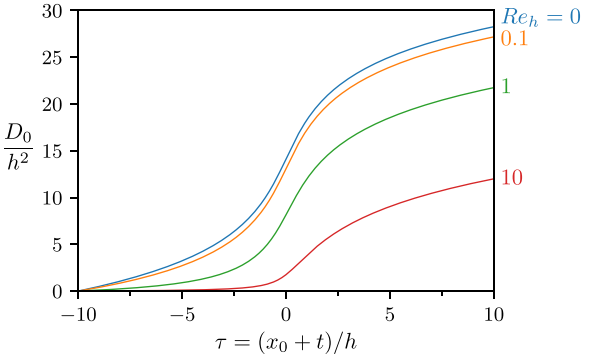


FIG. 4. The leading order drift volume $D_0(\tau;\tau_0,\mathrm{Re}_h)$ normalized by $h^2$ for Re $\ll 1$, as given by (20), where we have set $\tau_0 = -10$. The value of $\mathrm{Re}_h$ is indicated to the right of each curve.

result for Stokes flow. Indeed, (15) is recovered asymptotically from (20) as $\mathrm{Re}_h \to 0$ because the Stokes region grows unboundedly large in this limit. To show this formally, we see that if $\mathrm{Re}_h u \ll 1$, then the first bracketed term in (20) approaches unity while the second term yields $E_1(\mathrm{Re}_h u/4) \sim -\ln u(\tau) = \sinh^{-1}\tau$. Thus, $D_0(\tau) \to -\ln u(\tau) = \sinh^{-1}\tau$ as $\mathrm{Re}_h \to 0$. When $\mathrm{Re}_h$ is nonzero but much less than unity, the Stokes region is finite in size but still large compared to $h$, and the majority of the marked fluid is completely contained by the Stokes region as long as $|\tau| < 1/\mathrm{Re}_h$. Hence, $D_0$ is only marginally different than the Stokes flow prediction in this case, as is observed in Fig. 4 for $\mathrm{Re}_h = 0.1$.

As $\mathrm{Re}_h$ increases, the Stokes region becomes smaller compared to the height of the marked fluid, and inertia has an increasing effect on $D_0$. From Fig. 4, it is apparent that there is an overall decrease in $D_0/h^2$ with increasing $\mathrm{Re}_h$, or, equivalently, a decrease in $D_0$ with increasing Re given a fixed value of $h$. The reason is that the regions of flow that are dominated by viscous forces shrink in extent as Re is increased; the radius of the Stokes region decreases as $1/\mathrm{Re}$, and the wake narrows as $1/\sqrt{\mathrm{Re}}$. These regions are of utmost importance to generating drift because they are characterized by a velocity disturbance that exhibits a slow $1/r$ decay and moves fluid in the same general direction as the sphere, even at large distances (Fig. 3). In the part of the Oseen region outside of the wake, inertia causes the velocity to drop off more rapidly as $1/r^2$, and this much weaker flow contributes comparatively little to the drift volume.

Important differences between the nature of the drift volume at finite Re and that at $\mathrm{Re} = 0$ arise from the breaking of the fore-aft flow symmetry by fluid inertia. The asymmetry is greatest in the Oseen region due to the presence of the wake, and thus the influence of inertia is felt most when the majority of the marked fluid resides here, i.e., when $\mathrm{Re}_h \geqslant O(1)$. In contrast, the Stokes region makes a symmetric contribution to the drift volume that fades away as $\mathrm{Re}_h$ is made large. Equation (20) reveals that $\Delta(\tau) \neq -\Delta(\tau_0)$, whereas this inequality is an equality for inviscid and Stokes flows due to their fore-aft symmetry. Because the flow disturbance inside the wake is significantly stronger than that in the remainder of the Oseen region, the drift volume accumulated for $\tau > 0$ (i.e., after the sphere has passed through $x = 0$) is significantly greater than that for $\tau < 0$, and it becomes increasingly so as $\mathrm{Re}_h$ is increased (Fig. 4).

Furthermore, the slowly decaying velocity disturbance in the wake ($v \sim 1/r$) causes the marked fluid to be displaced an infinite distance, $X \sim \ln(\tau)$, as $\tau \to \infty$. The height of the wake diverges with the distance downstream, albeit slowly, as $w \sim \sqrt{|\hat{x}|/\mathrm{Re}}$. As a result, all of the marked fluid is eventually entrained by the wake as $\tau \to \infty$, regardless of the value of $\mathrm{Re}_h$. Therefore, the logarithmic divergence of $D$ as $\tau \to \infty$, found also for Stokes flow, persists at finite Re as the sphere passes far ahead of the $x = 0$ plane. Assuming that $\mathrm{Re}_h \geqslant O(1)$, the majority of the marked fluid is outside of the Stokes region and entrained by wake once $\tau \geqslant O(\mathrm{Re}_h)$. Thus, we find from (20) that $D_0 \sim \ln\tau$ for $\tau \gg \mathrm{Re}_h$, since $u(\tau) \sim 1/2\tau$ for $\tau \gg 1$.

However, $D$ converges as $\tau_0 \to -\infty$ at finite Re, unlike at $\mathrm{Re} = 0$, where it is divergent. In Stokes flow, the symmetric logarithmic divergence of $D$ as $\tau \to \infty$ and as $\tau_0 \to -\infty$ is due to the fore-aft flow symmetry. Viscous forces dominate everywhere if $\mathrm{Re} = 0$, and hence $v \sim 1/r$ everywhere far downstream and upstream of the sphere. Such symmetry is not present if Re is finite. Although viscous forces remain important far downstream in the wake, they become negligible everywhere else in the Oseen region, where $v$ drops more rapidly as $1/r^2$. Consequently, fluid elements upstream of the wake are not displaced nearly as far, and $D_0$ converges as $\tau_0 \to \infty$. For $\tau_0 \ll -1$, $u(\tau) \sim -2\tau$, and thus (20) shows that $\Delta_0(\tau_0) \sim -2/(\mathrm{Re}_h\tau_0) - C \to -C$ as $\tau_0 \to -\infty$. Interestingly, this reveals that the constant $C$ represents $D(\tau = 0; \tau_0 \to -\infty, h)$, which is finite.

## VI. POINT SOURCES OF MOMENTUM AND WAKES

At distances much greater than its radius, the sphere appears as a steady, translating point source of momentum (or vorticity) in an otherwise quiescent fluid, even if $\mathrm{Re} \geqslant O(1)$, granted that Re is not so large as to render the steady, axisymmetric flow unstable. In this case, the far-field flow is described by a steady Oseenlet of strength proportional to the external force $F = F(\mathrm{Re})$ required

to tow the sphere [34], where $F$ is normalized by $\varrho U^2 a^2$. This ignores the details of the flow in the immediate neighborhood of the sphere, but they are evidently unimportant for making a leading-order approximation to $D(\tau;\tau_0,h)$ when $h \gg 1$, since doing so only requires knowledge of $\psi$ at $r \geqslant O(h)$. At these far distances, the streamlines are nearly straight and parallel ($\rho \approx 1$). Therefore, for $h \gg 1$,

$$\psi_* \sim \frac{F}{4\pi}\left(1+\frac{\tau}{\sqrt{\tau^2+1}}\right)\left\{1-\exp\left[-\frac{\mathrm{Re}_h}{4}(\sqrt{\tau^2+1}-\tau)\right]\right\}. \tag{21}$$

Inserting (21) into (5), making the substitution $u = \sqrt{\tau^2+1}-\tau$, and integrating (omitting the $O(1)$ contribution by $\bar{V}_b(\tau)$) gives

$$\Delta_0 = \frac{F\mathrm{Re}h^2}{8}\left[\frac{1-\exp\left(-\frac{1}{4}\mathrm{Re}_h u\right)}{\frac{1}{4}\mathrm{Re}_h u}+E_1\left(\frac{1}{4}\mathrm{Re}_h u\right)\right]-C, \tag{22}$$

where $C = D(\tau=0;\tau_0\to-\infty,h)$ and is given by

$$C = \frac{F\mathrm{Re}h^2}{8}\left[\frac{1-\exp\left(-\frac{1}{4}\mathrm{Re}_h\right)}{\frac{1}{4}\mathrm{Re}_h}+E_1\left(\frac{1}{4}\mathrm{Re}_h\right)\right].$$

The $\mathrm{Re} \ll 1$ result (20) is readily recovered from (22) upon setting $F$ to the Stokes drag, $12\pi/\mathrm{Re}$. However, we also expect (22) to be valid for $\mathrm{Re} \geqslant O(1)$. Moreover, (22) apparently describes the leading-order drift volume induced by an arbitrarily shaped body as long as the far-field flow can be described by a steady Oseenlet. This will be the case as long as the body is towed by a steady external force acting along the direction of translation (i.e., there is a drag force but no lift force acting on the body). In describing the body as a point force, its dimensions are assumed to be small enough compared to the extent of the marked fluid that its exact geometry does not matter.

It follows that many of the details concerning the behavior of $D$ for $\mathrm{Re} \ll 1$ discussed in Sec. V remain pertinent for $\mathrm{Re} \geqslant O(1)$, except that now we must have $\mathrm{Re}_h \gg 1$, since (22) only applies if $h \gg 1$. The Stokes region existing at $\mathrm{Re} \ll 1$ is thus irrelevant; it disappears into the region near the sphere where the Oseenlet does not offer a valid description of the flow. In reality, viscous forces and the vorticity they generate are confined to a thin boundary layer adjacent to the sphere surface, of thickness $1/\sqrt{\mathrm{Re}}$, as Re becomes large. The only exception is the viscous wake, into which the vorticity is eventually shed and convected downstream by the bulk flow. Far from the sphere, the velocity disturbance in the wake decays as $1/r$, which we have already found to cause $D$ to eventually exhibit a logarithmic divergence with $\tau$ as $\tau \to \infty$.

It is possible to employ a boundary layer analysis to provide an additional description of the flow in the wake alone [29]. The sphere is again treated as a momentum point source, but streamwise vorticity diffusion is neglected in favor of the much stronger streamwise convection. Again assuming that $h$ is sufficiently large such that $\rho \approx 1$, this approximation to the flow yields

$$\psi_* \sim \frac{F}{2\pi}\left[1-\exp\left(-\frac{\mathrm{Re}_h}{8\tau}\right)\right]. \tag{23}$$

Putting (23) in (5), the contribution of the wake to the drift volume is

$$D_w(\tau) = \frac{F\mathrm{Re}h^2}{8}\left[\frac{1-\exp\left(-\mathrm{Re}_h/8\tau\right)}{\mathrm{Re}_h/8\tau}+E_1\left(\frac{\mathrm{Re}_h}{8\tau}\right)\right], \tag{24}$$

where we have taken $\tau_0 \to 0$ since (23) applies only to the downstream far-field flow. Normalizing the results from (22) and (24) by $F\mathrm{Re}h^2$ collapses them onto single curves for a given a value of $\mathrm{Re}_h$, and such curves are plotted in Fig. 5.

Comparing (24) to (22), it is readily verified that $D \sim D_w$ for $\tau \gg 1$ (recall that $u \sim 1/2\tau$), reaffirming our earlier statement that the wake dominates the drift whenever $\mathrm{Re}_h \gg 1$. Figure 5 accordingly reveals good agreement between the full Oseen approximation to $D$ and $D_w$ for $\tau \gg 1$,

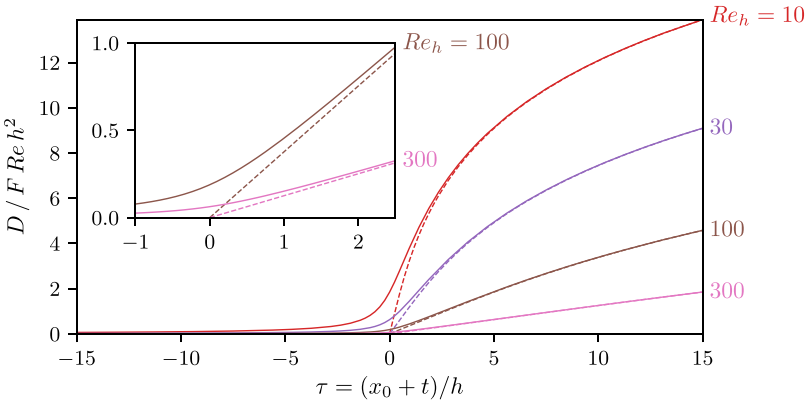


FIG. 5. The drift volume $D(\tau)$ for various values of $\mathrm{Re}_h \gg 1$, where we have taken $\tau_0 \to -\infty$. Normalizing $D$ by $F\mathrm{Re}h^2$ collapses $D$ to a single curve for each value of $\mathrm{Re}_h$. The solid lines show the result of the Oseen prediction (22), and the dashed lines correspond to the drift due only to the wake $D_w$ from (24). The values of $D$ and $D_w$ agree well for $\tau \gg 1$, but not for $\tau \leqslant O(1)$, as shown by the inlay.

even though (24) makes no prediction of the drift due to the flow outside of the wake. This is due to the fact that the flow outside the wake is relatively weak, and becomes increasingly so as $\mathrm{Re}_h$ increases. As a result, the agreement between $D$ and $D_w$ improves as $\mathrm{Re}_h$ is made larger. Additionally, it is apparent from Fig. 5 that there exists a regime in which $D$ increases linearly with $\tau$ given that $\mathrm{Re}_h$ is sufficiently large. Specifically, this regime occurs when $1 \ll \tau \ll \mathrm{Re}_h/8$. Here, the exponential term in (23) may be neglected, giving $\psi_* \sim F/2\pi$. It follows that $D_w \sim Ft$, and thus the drift volume due to the wake increases approximately linearly with time at a rate equal to $F$. Indeed, a simple momentum deficit argument suggests this relationship [8,9]; the momentum imparted on the fluid by the sphere must equal the total momentum deficit in the wake, independently of the distance downstream. Thus, $F = Q$, where $Q$ is the total flux through the wake normalized by $Ua^2$ [29]. When $\tau \ll \mathrm{Re}_h/8$, the marked fluid fully spans the wake ($w|_{x=0} \ll h$). Therefore, $D(t) \sim D_w(t) \sim \int^t Q dt = Ft$. On the other hand, when $\tau \geqslant O(\mathrm{Re}_h/8)$, the marked fluid is entirely entrained by the wake ($w|_{x=0} \geqslant O(h)$), and the linear increase of $D$ with $\tau$ becomes logarithmic as $\tau$ becomes significantly larger than $\mathrm{Re}_h/8$.

However, the reason why $D \not\sim D_w$ when $0 < \tau \leqslant O(1)$, as illustrated by the inlay in Fig. 5, is not immediately obvious since the velocity profiles in the wake provided by the Oseenlet and the boundary layer approximation closely coincide [34]. Importantly, the Oseenlet describes the entire far-field flow, rather than just that in the wake. Considering more carefully the flow due to the full Oseenlet, we gather from (21) that $\psi_* \sim F/4\pi$ when $|\tau| \ll 1$, and hence $D \sim Ft/2 = D_w/2$. This astonishingly suggests that $D$ increases at the *same* constant rate before *and* after the sphere crosses $x = 0$, despite the asymmetric nature of the flow field at finite Re due to the strong inward flux through the wake. Evidently, the wake does not make the only important contribution to $D$ when $|\tau| \leqslant O(1)$. The wake alone increases $D$ at a rate of approximately $F$ when $\tau \leqslant O(\mathrm{Re}_h/8)$. However, conservation of mass dictates that the flux through the wake $Q$ must be compensated by a source flow of equal strength emanating from the sphere [29] (Fig. 3). Since $w|_{x=0} \ll h$ when $\tau \leqslant O(1) \ll \mathrm{Re}_h$, only a small portion of the marked fluid actually resides in the wake in this case. The rest is well outside the wake, where the flow is indeed sourcelike [33]. After the sphere crosses $x = 0$ ($\tau > 0$), half of the source flow is directed backward toward $x = 0$. Since any fluid crossing backward though the $x = 0$ plane (for $0 < y < y_* \approx h$) contributes negatively to $D$, the source flow decreases $D$ at a rate of about $F/2$. It follows that $D \sim D_w - Ft/2 = Ft/2$. Before the sphere crosses $x = 0$ ($\tau < 0$), the half of the source flow that is directed ahead of the sphere (toward $x = 0$) similarly increases $D$ at a rate of about $F/2$. Here, the wake obviously does not contribute to $D$, and thus it is again found that $D \sim Ft/2$. Thus, despite its faster $1/r^2$ velocity decay, the sourcelike flow

outside of the wake still makes an appreciable contribution to $D$ when $|\tau| \leqslant O(1)$. As $\tau$ becomes larger, the effect of the source flow fades away, and only the drift induced by the wake remains important.

Yet again, $D$ critically depends upon what values that $\tau$ and $\tau_0$ are assumed to have. Thus, the details of how $D$ behaves as a function of $\tau$ and $\tau_0$ are important in predicting the results of experiments designed to measure the drift volume. If the length traveled by the body is large compared to $h$, such that the body passes far beyond the $x = 0$ plane ($\tau \gg 1$), then $D$ is almost entirely accounted for by the forward flux of fluid through the wake. However, if one takes $h$ to be comparable to or larger than the travel length ($\tau \leqslant O(1)$), then both the flux through the wake and the compensating source flow contribute to $D$. The non-absolutely-convergent behavior of $D$ is analogous to the similar happenings in inviscid flow and Stokes flow that are discussed in Secs. III and IV, respectively. However, the (far-field) flow pattern at finite Re is more intricate than the simple fore-aft symmetric flow patterns in these other cases, and the more complicated behavior of $D$ reflects this.

## VII. DISCUSSION

The preceding results for the drift volume are derived assuming that the flow in the comoving frame is steady everywhere. However, if the sphere is initially started from rest at $t = 0$, consideration must be given to the time it takes for the steady flow to fully develop. If $\mathrm{Re} \ll 1$ and we are only concerned with the flow up to the Oseen distance $r = O(1/\mathrm{Re})$, then the transient flow is governed by the unsteady Stokes equations. The dimensionless time scale $t_d$ for the momentum (or vorticity) to diffuse a distance $r$ from the sphere is $t_d \sim \mathrm{Re}r^2$. Thus, we expect the flow to be quasisteady for $r \ll \sqrt{t_d/\mathrm{Re}}$, and steady flow is approached as $t^{-1/2}$ [35]. For the prediction of the drift volume in steady Stokes flow given by (16) to apply, the time required for momentum to diffuse far past the marked fluid must be much shorter than the total travel time $t$ of the sphere. At $t = 0$, the distance to the furthest marked fluid element is approximately $\sqrt{x_0^2 + h^2}$. Thus, we have the condition that $t \gg \mathrm{Re}(x_0^2 + h^2)$.

As vorticity surpasses the Oseen length, it is transported via convection into the viscous wake (the remainder of the Oseen region remains irrotational). The wake grows diffusively in the transverse direction, but grows convectively (linearly) in the streamwise direction [36]. Therefore, the wake is bounded by an edge at an $O(t)$ distance downstream of the sphere. Similar dynamics apply to laminar wakes at larger Re. Thus, we expect that (22) and (24) accurately represent $D(t; x_0, h)$ only when the marked fluid is sufficiently far in front of the edge of the wake such that the flow there is approximately steady; i.e., the wake must be well developed.

A second source of unsteadiness occurs due to flow destabilization when Re is increased beyond a critical value. For a rigid sphere, unsteadiness first develops at $\mathrm{Re} \approx 210$ [37], inducing a time-dependent drag and lift force on the sphere. Further increases in Re lead to more complex temporal behavior, eventually triggering the transition to turbulent flow [38]. This clearly limits the applicability of the drift volume estimate given by (22) and (24), which strictly applies only if Re is sufficiently small for the flow to be steady and axisymmetric. However, if the time-averaged drag on the body is nonzero, it follows that there must also be a time-averaged momentum (and thus mass) deficit in the wake. Moreover, for three-dimensional flows, turbulent wakes eventually transition back to a laminar state at very far distances downstream [29]. This implies that the drift volume will still diverge with time (eventually logarithmically), even in the unsteady case, as long as there is a finite drag on the body.

It is interesting to consider the idealized case of a nondeformable spherical bubble with a perfect-slip surface translating steadily at $\mathrm{Re} \gg 1$. Because only an $O(1)$ amount of vorticity is generated in the boundary layer adjacent to the bubble, the flow remains steady and laminar, becoming irrotational as $\mathrm{Re} \to \infty$ [39]. The leading-order drag on the bubble is found to be $F \sim 48\pi/\mathrm{Re}$ [40]. As $\mathrm{Re} \to \infty$, it is reasonable to expect that the inviscid flow result for $D$ given by (9) should be recovered. However, as $\mathrm{Re}_h \to \infty$ in (22), the coefficient in front of the bracketed terms approaches a constant equal to $6\pi$ while the bracketed terms themselves vanish. Thus, we find instead that

$D \to 0$ as $\mathrm{Re} \to \infty$. This (lack of) prediction of $D$ by (22) is simply due to its leading-order nature. Treating the sphere as a point source of momentum neglects the fact that the body occupies a nonzero volume ($V_b$). As is shown in Sec. III, $D$ is $O(V_b)$ in inviscid flow.

Considering the simplified case of a single object translating through an unbounded fluid has been useful in understanding the fundamentals of how the drift volume is affected by fluid inertia. However, in real systems, other factors such as the existence of boundaries or multiple bodies in the flow may become important to the drift. In the case of external boundaries, it has been shown that, in Stokes flow, $D$ remains bounded as $t \to \infty$ even if only a single boundary is present [16,31,41]. The boundary triggers a velocity perturbation decay that is faster than $1/r$ ($1/r^2$ for a boundary parallel to the travel path, and $1/r^3$ for a perpendicular boundary) at some distance from the body. Furthermore, at finite Re, the presence of boundaries or other bodies in the fluid triggers the process of vorticity annihilation, which reduces the flux through the wake and leads to a reduced drift volume [16,42]. There are, of course, other possible situations which cause the velocity to decay more quickly than $1/r$ in the far field, such as density stratification of the fluid. There is the potential for much more work to be done in order to quantify drift and the drift volume in these scenarios.

Finally, it is important to mention that we have only examined the drift volume in the case that the body is towed steadily through the surrounding fluid by an external force (e.g., sedimenting particles or rising bubbles). If the body is self-propelled and free of acceleration and external forces, i.e., a neutrally buoyant swimmer, there are important differences in the far-field flow pattern that will greatly affect the induced drift volume. Within the Stokes region of a swimmer at $\mathrm{Re} \ll 1$, the flow is described by a stresslet ($v \sim 1/r^2$) rather than a Stokeslet ($v \sim 1/r$), and thus the far-field flow disturbance is much weaker compared to a towed body. At distances larger than the Oseen length, the flow disturbance in the wake behind a swimmer is also weaker than that of a towed body, having $v \sim 1/r^2$ and $v \sim 1/r^3$ inside and outside of the parabolic wake, respectively [43]. Moreover, it carries no net momentum (or mass) deficit because the swimmer is force free ($F = 0$) [8]. Clearly, the drift volume induced by a steady swimmer is essentially different from that due to an object translating under an external force.

## VIII. SUMMARY

We have conducted a detailed analysis of the drift volume $D(t; x_0, h)$ induced by a spherical body being steadily towed through an unbounded viscous fluid, where the flow around the sphere assumed to be steady and axisymmetric in the comoving frame. For simplicity, we only examined the case where the radius of the sphere is small compared to the extent of the marked fluid ($h \gg 1$). Our analysis was carried out by interpreting $D$ as the time-integrated flux through a kinematic plane that is stationary in the fixed frame and bounded by a stream tube in the comoving frame. A two-term asymptotic expansion of $D$ for $h \gg 1$ computed for Stokes flow ($\mathrm{Re} = 0$) revealed a positive $O(h)$ correction to $D$. This contrasts with the analogous result for inviscid flow, where this correction is $O(1/h^3)$ and negative. In addition, a leading-order result for $D$ at finite Re is computed, and its behavior as a function of travel time $t$ is shown to parametrically depend on $\mathrm{Re}_h = \mathrm{Re}h$.

A bounded drift volume for $t \to \infty$ and $h \to \infty$ is obtained only for the inviscid case, although the exact value of $D$ depends on the ordering of these limits. Otherwise, the drift volume generally diverges with both $t$ and $h$ as these quantities become large. However, the exact nature of this divergence critically depends upon the assumed ratio of the total distance traveled by the sphere to $h$, which is encapsulated by $\tau$ and $\tau_0$. The fact that evaluating $D(\tau; \tau_0, h \to \infty)$ amounts to evaluating the total momentum of the fluid (divided by $\varrho$) is responsible for this conditional behavior. Thus, if one wishes to experimentally measure $D$ for a body traveling in an effectively unbounded bulk fluid, the observed behavior may be expected to depend heavily on the values of $\tau$ and $\tau_0$. Our analysis yields the ability to predict $D$ in such experiments.

The drift volume induced by a body translating through a semi-infinite or fully bounded fluid domain at finite Re remains to be considered. The presence of boundaries is expected to have a profound impact on the induced drift volume, as is true for Stokes flow and inviscid flow. Furthermore,

the drift volume induced by self-propelled bodies, especially at finite Re, remains an area that is largely unexplored. The lack of a net external force on such swimmers will drastically alter the behavior of $D(t;x_0,h)$ compared to the result for a towed body. Finally, the drift volume due to unsteadily translating bodies appears to be another important area for future investigation. With regard to swimmers, most propel themselves in an unsteady manner. Examining this case therefore seems critical to understanding the physics of fluid transport by swimmers.

---


[1] P. J. Berenson, Experiments on pool-boiling heat transfer, Int. J. Heat Mass Transf. **5**, 985 (1962).
[2] I. Eames and M. A. Gilbertson, Mixing and drift in gas-fluidised beds, Powder Technol. **154**, 185 (2005).
[3] S. K. Kawatra and T. C. Eisele, Flotation column with adjustable supported baffles, U.S. Patent 5,335,785, August 9, 1994.
[4] E. H. Bouhabila, R. B. Aïm, and H. Buisson, Fouling characterisation in membrane bioreactors, Separ. Purif. Technol. **22-23**, 123 (2001).
[5] P. Cornel, M. Wagner, and S. Krause, Investigation of oxygen transfer rates in full scale membrane bioreactors, Water Sci. Technol. **47**, 313 (2003).
[6] K. Katija and J. O. Dabiri, A viscosity-enhanced mechanism for biogenic ocean mixing, Nature (London) **460**, 624 (2009).
[7] W. H. Munk, Abyssal recipes, Deep Sea Res. Oceanogr. Abstr. **13**, 707 (1966).
[8] G. Subramanian, Viscosity-enhanced bio-mixing of the oceans, Curr. Sci. **98**, 1103 (2010).
[9] A. M. Leshansky and L. M. Pismen, Do small swimmers mix the ocean? Phys. Rev. E **82**, 025301 (2010).
[10] D. O. Pushkin, H. Shum, and J. M. Yeomans, Fluid transport by individual microswimmers, J. Fluid Mech. **726**, 5 (2013).
[11] J. C. Nawroth and J. O. Dabiri, Induced drift by a self-propelled swimmer at intermediate Reynolds numbers, Phys. Fluids **26**, 091108 (2014).
[12] I. Eames and J.-B. Flór, Fluid transport by dipolar vortices, Dyn. Atmos. Ocean. **28**, 93 (1998).
[13] J. O. Dabiri, Note on the induced lagrangian drift and added-mass of a vortex, J. Fluid Mech. **547**, 105 (2006).
[14] S. Melkoumian and B. Protas, Wake effects on drift in two-dimensional inviscid incompressible flows, Phys. Fluids **26**, 123601 (2014).
[15] I. R. Peters, M. Madonia, D. Lohse, and D. van der Meer, Volume entrained in the wake of a disk intruding into an oil-water interface, Phys. Rev. Fluids **1**, 033901 (2016).
[16] I. Eames, The concept of drift and its application to multiphase and multibody problems, Philos. Trans. A. Math. Phys. Eng. Sci. **361**, 2951 (2003).
[17] S. Melkoumian and B. Protas, Drift due to two obstacles in different arrangements, Theor. Comp. Fluid Dyn. **30**, 529 (2016).
[18] L. Díaz-Damacillo, A. Ruiz-Angulo, and R. Zenit, Drift by air bubbles crossing an interface of a stratified medium at moderate Reynolds number, Int. J. Multiph. Flow **85**, 258 (2016).
[19] A. Prasad, J. Kondev, and H. A. Stone, Drift in supported membranes, Phys. Fluids **19**, 113103 (2007).
[20] W. J. M. Rankine, On plane water-lines in two dimensions, Philos. Trans. R. Soc. London **154**, 369 (1864).
[21] J. Clerk-Maxwell, On the displacement in a case of fluid motion, Proc. London Math. Soc. **s1-3**, 82 (1869).
[22] C. Darwin, Note on hydrodynamics, Math. Proc. Cambridge Philos. Soc. **49**, 342 (1953).
[23] C.-S. Yih, New derivations of Darwin's theorem, J. Fluid Mech. **152**, 163 (1985).
[24] C.-S. Yih, Evolution of Darwinian drift, J. Fluid Mech. **347**, 1 (1997).
[25] T. B. Benjamin, Note on added mass and drift, J. Fluid Mech. **169**, 251 (1986).
[26] I. Eames, S. E. Belcher, and J. C. R. Hunt, Drift, partial drift and Darwin's proposition, J. Fluid Mech. **275**, 201 (1994).
[27] J. Bataille, M. Lance, and J. L. Marie, Some aspects of the modeling of bubbly flows, in *Phase-interface Phenomena in Multiphase Flow (Proceedings of the International Centre for Heat and Mass Transfer)*, edited by G. F. Hewitt, F. Mayinger, and J. R. Riznic, Vol. 179 (Taylor & Francis, London, 1991).

[28] J. W. M. Bush and I. Eames, Fluid displacement by high Reynolds number bubble motion in a thin gap, Int. J. Multiph. Flow **24**, 411 (1998).
[29] G. K. Batchelor, *An Introduction to Fluid Dynamics* (Cambridge University Press, Cambridge, UK, 1967).
[30] M. E. Weber and D. Bhaga, Fluid drift caused by a rising bubble, Chem. Eng. Sci. **37**, 113 (1982).
[31] I. Eames, D. Gobby, and S. B. Dalziel, Fluid displacement by Stokes flow past a spherical droplet, J. Fluid Mech. **485**, 67 (2003).
[32] R. Camassa, R. M. McLaughlin, M. N. J. Moore, and A. Vaidya, Brachistochrones in potential flow and the connection to Darwin's theorem, Phys. Lett. A **372**, 6742 (2008).
[33] H. Lamb, *Hydrodynamics* (Cambridge University Press, Cambridge, UK, 1932).
[34] Y. D. Afanasyev, Wakes behind towed and self-propelled bodies: Asymptotic theory, Phys. Fluids **16**, 3235 (2004).
[35] A. B. Basset, *A Treatise on Hydrodynamics* (Deighton, Bell, and Co., Cambridge, UK, 1888), Vol. 2.
[36] P. M. Lovalenti and J. F. Brady, The hydrodynamic force on a rigid particle undergoing arbitrary time-dependent motion at small Reynolds number, J. Fluid Mech. **256**, 561 (1993).
[37] R. Natarajan and A. Acrivos, The instability of the steady flow past spheres and disks, J. Fluid Mech. **254**, 323 (1993).
[38] A. G. Tomboulides and S. A. Orszag, Numerical investigation of transitional and weak turbulent flow past a sphere, J. Fluid Mech. **416**, 45 (2000).
[39] L. G. Leal, Vorticity transport and wake structure for bluff bodies at finite Reynolds number, Phys. Fluids A: Fluid Dyn. **1**, 124 (1989).
[40] D. W. Moore, The boundary layer on a spherical gas bubble, J. Fluid Mech. **16**, 161 (1963).
[41] I. Eames, J. C. R. Hunt, and S. E. Belcher, Displacement of inviscid fluid by a sphere moving away from a wall, J. Fluid Mech. **324**, 333 (1996).
[42] J. C. R. Hunt and I. Eames, The disappearance of laminar and turbulent wakes in complex flows, J. Fluid Mech. **457**, 111 (2002).
[43] A. S. Khair and N. G. Chisholm, Expansions at small Reynolds numbers for the locomotion of a spherical squirmer, Phys. Fluids **26**, 011902 (2014).